Progress in Propulsion Physics **2** (2011) 285-296

CONSIDERATION OF REAL GAS EFFECTS AND CONDENSATION IN A SPRAY-COMBUSTION ROCKET-THRUST-CHAMBER DESIGN TOOL

M. Frey, B. Kniesner, and O. Knab

Astrium GmbH, Space Transportation
München D-81663, Germany

For the prediction of hot gas side heat transfer in rocket thrust chambers, Astrium Space Transportation (ST) uses the second generation multiphase Navier–Stokes solver Rocflam-II. To account for real-gas and condensation effects, pressure-dependent and even multiphase fluid data are included in the chemistry tables used by the code. Thus, the changing fluid properties near the two-phase region as well as transformation from gaseous to liquid and even solid state are reflected properly. Heat flux measurements for a dedicated subscale test campaign with strongly cooled walls show a clearly increasing heat load as soon as the combustion gases condense at the wall, due to the released latent heat of condensation. Corresponding coupled Rocflam-II/CFX simulations show a good quantitative agreement in heat flux for load cases with and without condensation, showing the ability of the code to correctly simulate flows in the real-gas and even inside the two-phase region.

1 INTRODUCTION

Astrium ST and its predecessor companies developed and manufactured rocket thrust chambers for more than forty years. In the early days, mainly Nusselt-based correlations were applied to predict the occurring wall heat fluxes and temperatures. A large number of subscale and full-scale tests were required to reach a consolidated design. Today, the application of computational fluid dynamics (CFD) simulations becomes more and more common during the development process of rocket engines, thereby reducing the number of required tests and saving resources. During the past five years, it has become state-of-the-art at Astrium ST to predict the heat transfer in rocket thrust chambers via coupled CFD simulations of the hot gas side and the coolant flow (conjugate heat transfer). A prerequisite for the correct prediction of heat transfer is the precise knowledge of the fluid properties for both combustion products and coolant.

Article available at http://www.eucass-proceedings.eu or http://dx.doi.org/10.1051/eucass/201102285

In the H_2/O_2 thrust chambers Vulcain 1 and Vulcain 2 designed during the past two decades by Astrium and its predecessor companies, the philosophy for the cooling channel design was to ensure structural integrity and flawless function of the thrust chamber at minimum coolant pressure loss over the specified lifetime. This resulted in thrust chamber wall temperatures well above the condensation temperature of water, which is the main combustion product in H_2/O_2 engines. In this temperature range, all combustion products are gaseous and their thermodynamic and transport properties do not depend on pressure. However, there are other engine configurations that inherently result in considerably colder thrust chamber walls. Two examples for such configurations are regenerative nozzles and expander-cycle thrust chambers, respectively. In the former, the cold walls are due to the fact that the full amount of available fuel is used to cool the nozzle, which is far more than would actually be required to guarantee the specified life time. In the latter, the attempt to extract as much as possible energy from the combustion gases in order to drive the turbines results in a very strong cooling. For such strongly cooled walls, the water steam in the combustion gases approaches the condensation line, and pressure-dependent real gas effects occur. The combustion gases can even condense or freeze at the cooled walls, as proved by a recently published American rocket engine test video of the Common Extensible Cryogenic Engine (CECE) based on the RL-10 expander design [1]. Here, liquid water and even ice can be observed at the exit of the nozzle.

As soon as such low wall temperatures are reached in thrust chambers, the standard modeling using pressure-independent fluid properties is no longer applicable. Therefore, Astrium has extended its standard coupled CFD approach for thrust chambers to be able to properly take into account real gas effects and even condensation. This paper describes the new method.

2 APPLIED TOOLS

Astrium follows different approaches to predict the heat transfer to the thrust chamber walls. On the one hand, the Nusselt-based engineering tool RCFS-II [2] is used mainly in the design process, delivering results within seconds of computational time. On the other hand, a more elaborate coupled CFD-approach is applied as soon as detailed analyses become necessary. The hot gas side and coolant side are simulated separately by two independent CFD tools, which are loosely coupled to each other. The wall temperature from the coolant simulation is prescribed as a boundary condition for the hot gas side simulations, and the heat flux from the hot gas side simulation is prescribed as a boundary condition for the coolant simulation.

For the hot gas side, Astrium applies the axisymmetric in-house multiphase Navier–Stokes code Rocflam-II, which is a merger from two previous in-house

codes, namely, CryoROC [3] and ROCFLAM [4]. While CryoROC treated problems with cryogenic propellants H_2 and LOx (liquid O_2), ROCFLAM was mainly used to model storable propellant problems, especially MMH/NTO (monomethylhydrazine / nitrogen tetroxide) thrust chambers. The second generation code Rocflam-II is able to treat problems with almost arbitrary propellants [5]. As its predecessors, Rocflam-II is an axisymmetric Navier–Stokes solver with a Lagrange droplet tracking module, offering different injection possibilities, depending on the thermodynamic state of the fluid.

For purely gaseous injection, the Lagrange module is switched off, and the propellants are injected through openings in the face plate. Alternatively, the gaseous components can be modeled as source terms in the conservation equations for mass, momentum, enthalpy, and concentration or mixture fraction without modeling wall opening.

For liquid rocket engine applications as the aforementioned Vulcain 1 and 2, this injection by source terms is applied for the H_2 fuel, where the injection temperature is clearly above the critical temperature. In contrast, the injection of LOx is realized via droplets in the Lagrange module, where the injection temperature, momentum, and lognormal droplet distribution is prescribed. An order of magnitude of 1 million droplet trajectories is tracked throughout the combustion chamber (CC), interacting with the gas phase and evaporating, which is modeled by source terms for mass, momentum, and energy in the Navier–Stokes solver. The volume of the liquid phase is neglected by the Navier–Stokes solver. The void fraction, representing the local volume fraction of the liquid phase, exceeds the usually applied critical value of 10% only very locally near the injection positions, which is considered to be acceptable. The injection of LOx as droplet in the Lagrange module is also used in case of supercritical pressure at subcritical temperature, although no surface tension and thus different phases exist for this case.

The axisymmetric code Rocflam-II is usually applied to three-dimensional (3D) injection configurations. For the axisymmetric simulation, the single injection elements are transferred into injection rings as shown in Fig. 1 for a subscale injection head with coaxial elements. When simulating a 3D configuration with an axisymmetric code and choosing an injection of the propellants as gases through wall openings, the problem occurs that with the higher assumed injection area (in Fig. 1, (a) is compared to (b)), a lower injection velocity results in order to maintain continuity. The injection without wall opening either as gaseous source terms (H_2) or through the Lagrange module (LOx) allows prescribing the correct injection mass flow and velocity and thus the correct injection momentum although the simulated injection area is different.

Rocflam-II includes two different chemistry models, both taking into account turbulent combustion. First, a global chemistry based on globally defined reactions is available, where the reaction rate is determined with an eddy-dissipation concept or Arrhenius formulation. For each species concentration, a dedicated

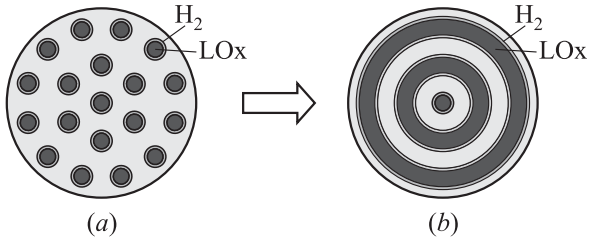

Figure 1 Scheme of an injection head with single coaxial injection elements (*a*) and realization in the axisymmetric code Rocflam-II (*b*)

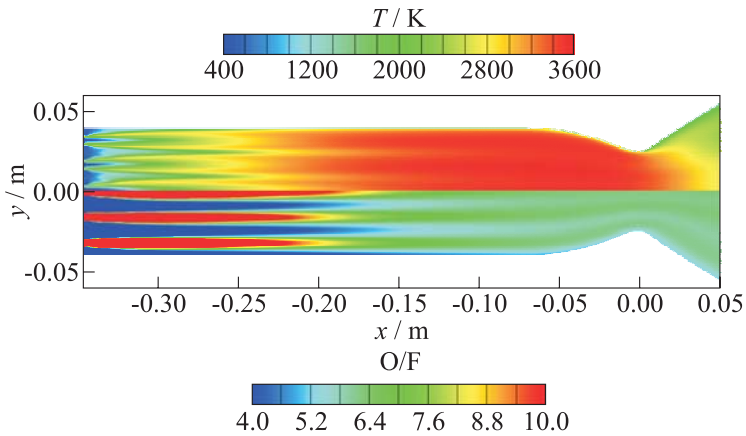

Figure 2 Simulation of a H_2/O_2 40-kilonewton combustor with Rocflam-II; static temperature (top), and O/F ratio (bottom). (Refer Freyet *et al.*, p. 288.)

differential equation is solved. Second, there is an equilibrium table-based chemistry model with a one-dimensional ppdf (presumed probability density function) approach taking into account the influence of turbulent combustion on the local oxidizer-to-fuel (O/F) ratio. No species concentration equations are solved, only a global mixture fraction and its variance are treated by differential equations. This latter approach is used today for simulating H_2/O_2 and methane/O_2 thrust chambers.

Figure 2 shows the simulation result for a typical H_2/O_2 subscale CC with 19 injection elements in three injection rows and wall temperature clearly above the water condensation temperature. The wall temperature was prescribed in this simulation; thus, no coolant side simulation was performed. As described before, hydrogen is injected as source term, whereas the supercritical LOx is tracked via the Lagrange module. The lower half of Fig. 2 presents the O/F ratio

with fully separated hydrogen and oxygen near the faceplate and more and more mixing towards the throat and exit. Note the propellants do not mix perfectly until the throat, resulting in a combustion efficiency below unity. The upper half of Fig. 2 shows the static temperature that can be used as indicator for the completeness of combustion. As expected, the static temperature increases in the streamwise direction as the propellants mix and decreases as the combustion gases are expanded through the throat and nozzle. A qualitative comparison of the simulation results with test data is shown in Fig. 3. As can be seen, the heat flux density compares well to the experimental data, except for a very small region near the face plate, where 3D effects might dominate the flow, which cannot be resolved by the axisymmetric code.

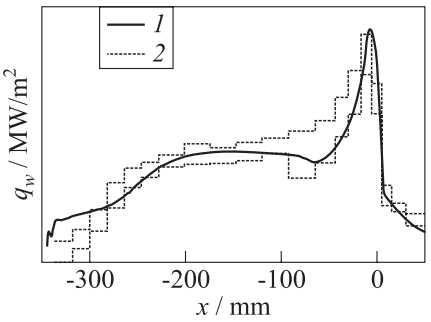

Figure 3 Comparison of numerical simulation (Rocflam-II) (*1*) and test data for the 40-kilonewton combustor (minimal and maximal heat flux) (*2*)

Unlike in the preceding example where the wall temperature was prescribed, usual rocket problems also require the modeling of the coolant side. Astrium uses the commercial 3D CFD-package ANSYS CFX to simulate the structure of thrust chamber wall and the flow inside the cooling channels. In order to reduce the computational effort, benefit is taken from existing symmetry or periodicity conditions, and only one cooling channel is simulated in 3D. In the case of cryogenic coolants, special pressure-dependent low-temperature data are provided to the code by a fluid data base including real-gas effects.

3 REAL-GAS EFFECTS IN H_2/O_2 THRUST CHAMBERS

Inside the core flow of CC and nozzle, the combustion products can be characterized as a mixture of ideal gases, meaning that the density can be computed from pressure and temperature and that the enthalpy depends only on temperature, but not on pressure. Of course, density and molar mass of the mixture have to be applied, and they can be computed using appropriate mixing rules based on mole fraction and molar mass of the individual gas components. Chemistry models can be applied to determine the composition of this gas mixture, which depends not only on the mixture ratio and temperature or enthalpy, but also on pressure. Thus, a suitable chemistry model and pressure-independent fluid properties of the components are sufficient to characterize the fluid properties of the mixture.

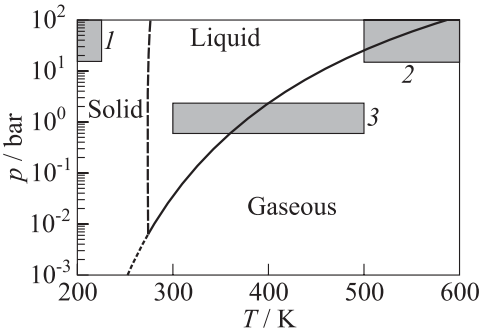

Figure 4 Phase diagram for water with regions for injection (*1*) and CC (*2*) and nozzle (*3*) walls

One of the most frequently used fluid properties data base, the so-called NASA-polynomials [6] also applied by the famous CEA-code [7], is pressure-independent as well. The NASA-polynomials were used by the predecessors of Rocflam-II, namely, CryoROC and ROCFLAM.

However, having a closer look at the thermodynamic state reveals that the assumption of pressure-independent fluid properties might not be valid everywhere in the chamber. Near the injection plane, temperatures not much above the injection temperature occur wherever the propellants have not yet reacted, and also at the cooled walls, moderate temperatures below 700 K and, hence, near-condensation temperature of water are reached. Figure 4 shows a phase diagram (pressure over temperature) for water where the possible pressure–temperature combinations for H_2/O_2 rocket thrust chambers are shown. As can be seen, the condensation line can be passed for these cases resulting in the occurrence of liquid water or even ice; hence, the ideal gas assumption loses its validity.

A more detailed look on real-gas behavior near the condensation line is given in Fig. 5, where a temperature–entropy (T–S) diagram for water is shown (note that the absolute values of enthalpy are arbitrary, depending on the chosen zero value). For an ideal gas, enthalpy only depends on temperature; hence, enthalpy lines are horizontal lines in the T–S diagram. This is not the case for water steam

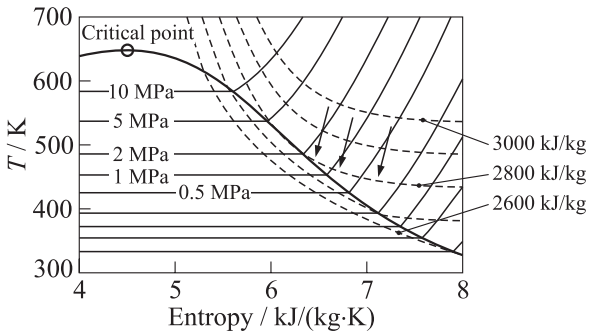

Figure 5 T–S diagram for water, including enthalpy (dashed) and pressure (solid) isolines

as the two-phase region is approached (see, e. g., the enthalpy isoline marked by the arrows in Fig. 5). This means that even without the actual occurrence of condensed water, a real-gas behavior is observed, which must be taken into account for modeling.

4 IMPLEMENTATION OF REAL-GAS EFFECTS IN ROCFLAM-II

The basis of the equilibrium-based ppdf chemistry model is the so-called chemistry table, which contains values for temperature, density, molar mass, species concentrations, and the transport properties as functions of enthalpy, pressure, and mixture fraction. Considering H_2/O_2 combustion, at high mixture temperatures, the composition and all fluid properties are taken from CEA [7], reflecting the chemical equilibrium state. At low temperatures, the combustion gases are assumed to consist only of H_2O and H_2 for fuel-rich and H_2O and O_2 for oxidizer-rich cases and the pressure-dependent properties are taken from a fluid data base including real-gas and two-phase effects. Note that H_2O can — depending on its partial pressure and temperature — occur as steam, liquid water, ice, or a combination of them. A two-dimensional excerpt from the 3D chemistry table is shown in Fig. 6. As an example, the value of temperature is shown as a function of mixture fraction f and enthalpy h at a given constant pressure. The two-phase regions (gaseous–liquid and liquid–solid) can be seen as discontinuities, which are plateaus at the stoichiometric mixture fraction, but smear out towards mixture fraction values of zero (only oxygen) and unity (only hydrogen).

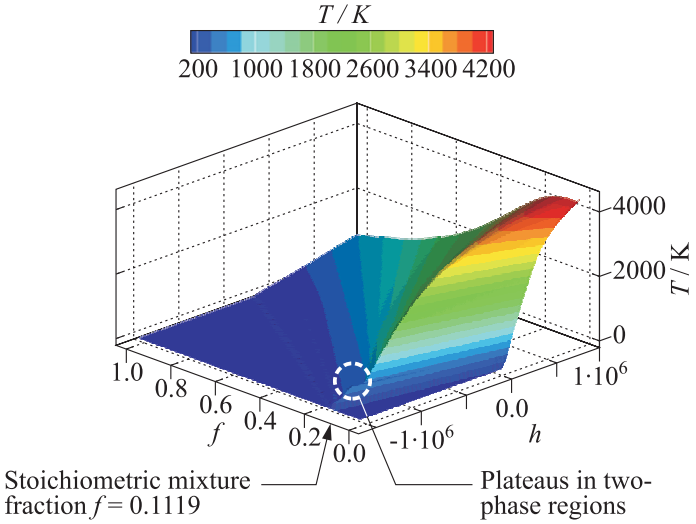

Figure 6 Temperature as a function of mixture fraction f and enthalpy h extracted from the Rocflam-II chemistry table at constant pressure; note the absolute values of enthalpy are arbitrary. (Refer Frey *et al.*, p. 291.)

Within Rocflam-II, the values of enthalpy, pressure, and mixture fraction are computed by dedicated differential equations. Taking all other fluid properties from the respective point in the chemistry table would result in a pure chemical equilibrium solution. However, the variance of the mixture fraction is also computed by a differential equation, influenced strongly by turbulence parameters. Rocflam-II now evaluates the chemistry table not only at one specific mixture fraction, but at different mixture fraction values, dispersed around the actually computed value following the chosen pdf function and weighted accordingly in order to reflect the influence of turbulent combustion.

The method explained above allows correct simulation of gaseous flows near the two-phase region, where real-gas effects occur. This is important for accurate heat flux computations at regeneratively cooled walls even if the condensation limit is not reached. In addition, the simulation of flows with the occurrence of condensation is possible. The occurring water is then treated as a dense gas without considering surface effects as they occur in liquids. As a consequence, liquid water and gaseous components mix perfectly and do not occur as droplets, bubbles, or film, respectively. Note that the basis for the modeling is the equilibrium assumption which seems to be justified by the low velocities in the boundary layer and the presence of the wall that acts as condensation nucleus. It is emphasized that the release of latent heat of condensation is correctly reflected as well as the considerable change in density values and transport properties. This prediction capability is important for accurate heat load management within a rocket CC and nozzle.

5 APPLICATION OF ROCFLAM-II TO A CASE WITH CONDENSATION

A dedicated subscale campaign was performed to investigate real-gas effects and condensation in the divergent section of rocket thrust chambers. For this purpose, a hydrogen-cooled copper thrust chamber was built with a maximum expansion ratio above 15. A partly conical nozzle contour was chosen due to manufacturing reasons. During the tests, the coolant mass flow was varied, resulting in a wall temperature variation from clearly above the condensation limits to values clearly below.

In order to get correct values of the resulting wall temperature in a thrust chamber cooled via channels, the Rocflam-II hot-gas side simulation was loosely coupled to a 3D CFX coolant side simulation, including structure and cooling channel flow. In this coupling, the wall heat flux from an initial Rocflam-II simulation was prescribed as a boundary condition for the coolant side simulation. In turn, the wall temperature calculated by the coolant side simulation was set as a boundary condition for the next Rocflam-II simulation. This procedure was repeated until a converged wall temperature was reached, possibly supported

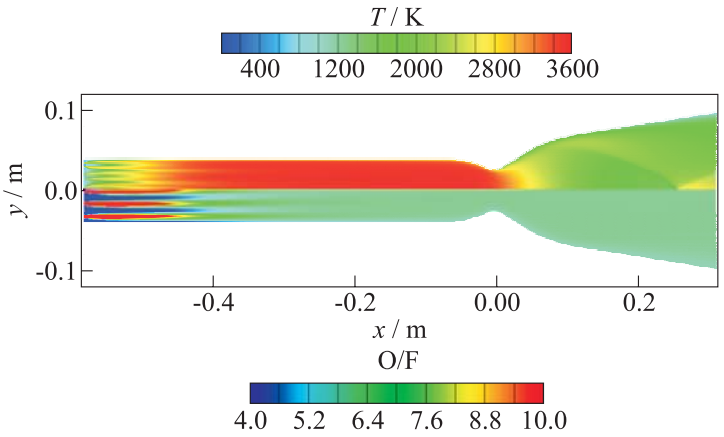

Figure 7 Coupled Rocflam-II/CFX simulation of an elongated subscale thrust chamber (hot gas side); top: static temperature; bottom: O/F ratio. (Refer Frey *et al.*, p. 293.)

by some underrelaxation. Coupled Rocflam-II/CFX simulations were performed for selected load points, differing only in coolant mass flows and thus wall temperature. An isoplot of the hot gas side is shown in Fig. 7, displaying static temperature and local O/F ratio. The global behavior is comparable to that of the 40-kilonewton subscale thruster shown above in Fig. 2; however, the longer cylindrical CC section and the different nozzle shape mark clear differences. The strong contour curvature upstream of the conical nozzle induces compression waves focusing to a weak shock without further influencing the wall flow. Figure 8 shows the corresponding cooling channel simulation with CFX, displaying the coolant velocity as isoplot.

Figure 9*a* shows the wall temperature distribution resulting from the simulation of the subscale thrust chamber for different coolant mass flows at identical chamber pressure and O/F ratio. Condensation occurs as soon as the wall temperature drops below the condensation temperature which is a function of the partial pressure of water steam in the combustion gases. The test with a coolant mass flow rate of 42% shows no condensation, whereas all other cases do. As expected, the wall temperature decreases with increasing coolant mass flow, but the decrease becomes weaker as the wall temperature drops below the condensation temperature due to the released heat of condensation acting as a heat source. As can be seen from Fig. 9*b*, a considerable increase in heat flux is indeed visible as condensation occurs, again a result of the released heat of condensation. The fact that the specific heat flux is very sensitive to the occurrence of water whereas the wall temperature is not, implies that the comparison to experimental data should be performed in terms of heat flux rather than in terms

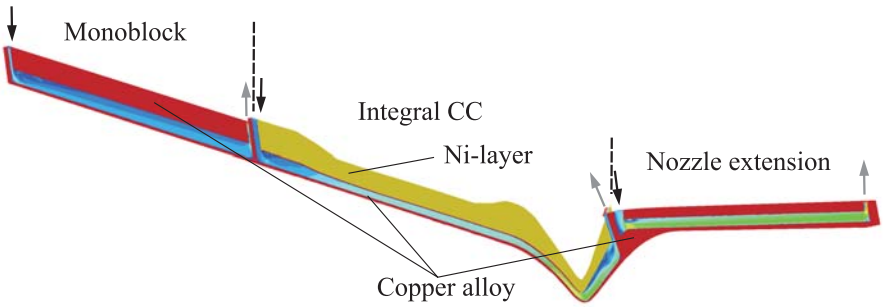

Figure 8 Coupled Rocflam-II/CFX simulation of an elongated subscale thrust chamber (coolant side); coolant velocity is shown as isoplot. (Refer Frey *et al.*, p. 294.)

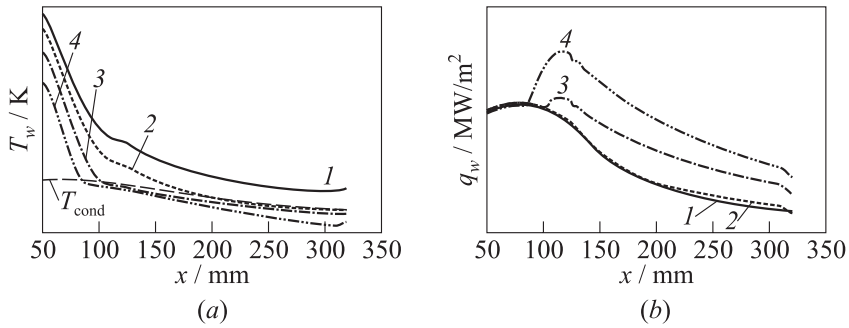

Figure 9 Wall temperature (*a*) and specific heat flux (*b*) for four different coolant mass flows (coupled Rocflam-II/CFX simulation): *1* — 42% cooling; *2* — 53%; *3* — 74%; and *4* — 100% cooling

of wall temperature, which is additionally supported by the great difficulties in measuring correct wall temperatures.

In the subscale tests, only the integral heat flux for the nozzle segment was measured by analyzing the coolant enthalpy at inflow and outflow. This value is presented in Fig. 10 for various tests by circles, showing a considerable increase with cooling rate and thus decreasing wall temperature (solid line). In flows without condensation, the same trend (higher heat flux for lower wall temperature) is visible, but at a much lower slope, represented by the dashed line. The explanation for the considerable increase of integral heat flux is again the released latent heat of condensation which increases with coolant rate. Note that for the presented subscale tests, the increase in integral heat flux due to condensation is as high as 80%. In addition to the measured values, Rocflam-II simulation results are shown in Fig. 10 as squares, indicating a very good agreement to test data for cases without (cooling rate 42%) as well as with condensation (cooling rate 53%,

74%, and 100%). This confirms the ability of the chosen approach not only to correctly predict the occurrence of condensation, but also to predict the heat flux with good accuracy. Such prediction capability is only possible if the accuracy of the simulated wall temperature is high, which requires thoroughly validated tools for the hot gas as well as the coolant side.

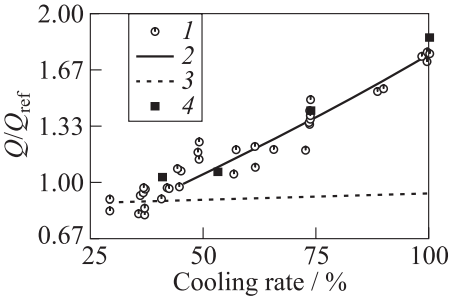

Figure 10 Comparison of measured and simulated integral heat fluxes for the subscale thrust chamber: *1* — test data; *2* — fit for data with condensation; *3* — fit/extrapolation for data without condensation; and *4* — Rocflam-II/CFX

As a part of the Rocflam-II solution, the amount of condensed water is available for arbitrary cross sections of the thruster. However, a validation to test data of the water mass flow itself is not possible because no such measurements are available. However, the good agreement in terms of integral heat pickup represents some indirect validation also for the simulated amount of water.

6 CONCLUDING REMARKS

In contrast to combustion chambers for gas-generator cycles and dump-cooled nozzles, where resulting wall temperatures usually are above the critical point of water, expander-cycle thrust chambers and regenerative nozzles show considerably lower wall temperatures where real-gas effects can no longer be neglected. Classical tools using pressure-independent fluid data fail in the prediction of wall heat flux for these applications. The second generation spray-combustion tool Rocflam-II, however, is able to reflect the fluid data correctly in the vicinity of the two-phase region of water and even beyond, by introducing pressure-dependent and even two-phase data into the chemistry tables used for the equilibrium-based ppdf-approach. However, occurring water is modeled as a dense gas, correctly reflecting all thermodynamic and transport properties, but neglecting surface tension. Hence, water and steam mix perfectly, and typical effects of two-phase flows with surface tension, namely, the formation of droplets, bubbles, or closed films, cannot be reflected.

Coupled Rocflam-II/CFX simulations have been compared to dedicated subscale test data with subcooled walls to find out how far the occurring real-gas effects and even condensation are reproduced by this approach. Simulation as well as experimental data show a strong increase in heat flux as soon as condensation occurs, which is due to the released latent heat of condensation. The

comparison between simulation and test shows good quantitative agreement for different coolant mass flows and, hence, for cases with and without condensation. Consequently, Rocflam-II/CFX is suited well to predict the heat transfer for cases with cool CC or nozzle walls and can be applied in the design process of expander engines and regenerative nozzles in spite of the assumptions of the dense-gas approach.

Having reached this important step in modeling the real-gas behavior and condensation of water, the next step will be to investigate the influence of a liquid water film on the thrust chamber wall further downstream with a wall temperature exceeding the condensation temperature. In this case, the film evaporates, thereby consuming the latent heat of evaporation and cooling the warm structure. The first question to be solved in this context is whether the presented dense-gas approach assuming equilibrium phase change is suited also for the case of evaporation.

ACKNOWLEDGMENTS

Part of the presented work was performed within the European expander demo programme (part of FLPP), organized by ESA via Snecma. The authors thank Jean-Noël Caruana (ESA), Lionel Denis and Isabelle Jeaugey (Snecma) as well as Thomas Mattstedt and Dietrich Haeseler (Astrium) for the fruitful cooperation.

Special thanks are addressed to the Astrium colleagues Axel Preuß, responsible for the subscale tests, and Konrad Vollmer for test evaluation.

REFERENCES

1. http://www.nasa.gov/mission_pages/constellation/multimedia/cece.html
2. Maeding, C., D. Wiedmann, K. Quering, and O. Knab. 2011. Improved heat transfer prediction engineering capabilities for rocket thrust chamber layout. In: *Progress in propulsion physics*. Eds. L. DeLuca, C. Bonnal, O. Haidn, and S. Frolov. EUCASS advances in aerospace sciences book ser. TORUS PRESS, EDP Sciences. 2:239–50.
3. Knab, O., A. Fröhlich, J. Görgen, and D. Wiedmann. 2002. Advanced thrust chamber layout tools. *4th Conference (International) on Launcher Technology "Space Launcher Liquid Propulsion" Proceedings*. Liege, Belgium.
4. Knab, O., A. Fröhlich, and D. Wennerberg. 1999. Design support for advanced storable propellant engines by ROCFLAM analyses. AIAA Paper No. 99-2459.
5. Görgen, J., T. Aichner, and M. Frey. 2009. Spray combustion and heat transfer modelling in LOx/H_2, LOx/HC and MMH/NTO combustion chambers. *3rd European Conference for Aerospace Sciences (EUCASS)*. Versailles, France.
6. McBride, B., S. Gordon, and M. Reno. 1993. Coefficients for calculating thermodynamic and transport properties of individual species. NASA Technical Memorandum 4513.
7. Gordon, S., and B. McBride. 1994. Computer program for calculation of complex chemical equilibrium compositions and applications. NASA Reference Publication 1311.